SECED 2023 Conference
Earthquake Engineering & Dynamics for a Sustainable Future
14-15 September 2023, Cambridge, UK

SEISMIC FRAGILITY OF CODE-CONFORMING SINGLE-STORY RC PRECAST BUILDINGS CONSIDERING MULTIPLE FRAGILITY METHODS

Gennaro MAGLIULO[1], Danilo D'ANGELA[2], Valeria PICCOLO[3], Chiara DI SALVATORE[4] & Nicola CATERINO[5]

Abstract: *Seismic fragility curves represent an advanced tool for assessing seismic capacity of structures according to the performance-based earthquake engineering (PBEE) approach. However, several methods have been defined in the literature, and very few studies provide information regarding the influence of the different methods on the capacity estimations. Furthermore, fragility is often assessed considering ultimate limit performance levels and is referred to unique capacity criteria, especially for reinforced concrete (RC) precast buildings. The present study reports an extensive comparison of fragility curves assessed considering multiple fragility methods, i.e., Shome and Cornell (or 3 parameter, 3Par), maximum likelihood fit (MLF), normal probability paper (NPP), and least squares fit (LSF). The fragility curves are estimated by processing the results of multiple-stripe analysis (MSA) carried out considering advanced inelastic three-dimensional models. Both serviceability and ultimate limit states are considered, according to multiple damage response and capacity criteria. In particular, nonstructural damage, local rotational yielding, significant structural damage, brittle and ductile beam-to-column connection failure, and global collapse conditions are taken into account. The case study buildings consist in two layouts of single-story RC precast buildings, designed according to the current Italian building code over low-, medium-, and high-hazard sites in Italy, including two soil conditions. The study sheds light on the influence of the fragility method on the seismic capacity, as well as it characterizes the seismic response of the buildings correlating the capacities associated to multiple damage states. Finally, critical insights are supplied regarding the influence of the design provisions, towards the improvement of the current design/assessment approaches.*

Introduction

Reinforced concrete (RC) precast buildings typically host industrial and commercial facilities and have a major role for regional, national, and international economy. Single-story RC precast buildings are quite widespread in Italy and Europe, and their layout and structural details are quite similar among the different building assets. Current regulations (e.g., (British Standards Institution and European Committee for Standardization, 2005; Ministero delle Infrastrutture e dei Trasporti, 2018)) provide design methods, requirements, and structural detailing criteria to achieve adequate performance with regard to the seismic actions. However, these structures might exhibit an inadequate seismic capacity considering both serviceability and ultimate limit states (LSs), as it was highlighted in literature studies (e.g., (Cimmino et al., 2020; Clementi et al., 2016; Ozden et al., 2014; Toniolo and Colombo, 2012)). The seismic vulnerability of code-conforming RC precast buildings was assessed in the literature often considering unique damage criteria and/or considering ultimate LS conditions (e.g., (RINTC Workgroup, 2018)). Furthermore, no technical guidance is provided regarding the most efficient and reliability assessment methodology and fragility estimation formulations.

The present studies provide a comprehensive assessment of the seismic fragility of code-conforming single-story RC precast buildings, considering multiple geometry layout, seismic sites, and soil conditions. In particular, multiple fragility assessment techniques are implemented. The

1 Associate professor, University of Naples Federico II, Naples, Italy; Construction Technologies Institute, National Research Council, Naples, Italy, gmagliul@unina.it
2 Assistant professor, University of Naples Federico II, Naples, Italy, danilo.dangela@unina.it
3 Post-doc researcher, University of Parthenope, Naples, Italy
4 Post-doc researcher, University of Naples Federico II, Naples, Italy
5 Associate professor, University of Parthenope, Naples, Italy; Construction Technologies Institute, National Research Council, Milan, Italy

study is carried out in the framework of Italian National project DPC-ReLUIS RINTC (Iervolino et al., 2023, 2018; Iervolino and Dolce, 2018; Magliulo et al., 2023; RINTC Workgroup, 2018), and it develops novel knowledge and technical insights into the field, with a particular focus on operative applications.

Methodology

Case study buildings

The investigated buildings were derived from the common characteristics of one-story RC precast buildings designed/built over the Italian and European territory. The reference design code is the Italian building code NTC 2008 (Consiglio Superiore dei Lavori Pubblici (CS.LL.PP.), 2008), which is compliant with the current Italian building code NTC 2018 (Ministero delle Infrastrutture e dei Trasporti, 2018)and compatible with the Eurocode 8 (British Standards Institution and European Committee for Standardization, 2005). The geometric layout of the investigated buildings is depicted in Figure 1. In particular, two layout were considered: (SS) short-span, having L_1 and L_2 equal to 15.0 and 6.0 m, respectively, and (LS) long-span, having L_1 and L_2 equal to 20.0 and 8.0 m, respectively; for both SS and LS configurations, H and H_1 were equal to 9.0 and 7.5 m, respectively.

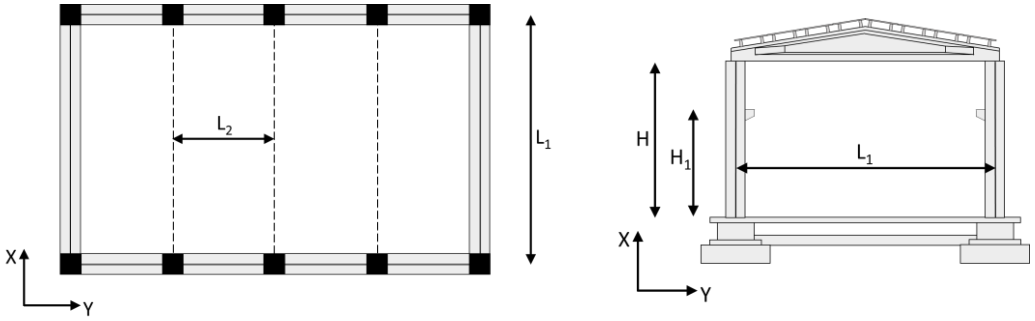

Figure 1. Geometric layout of the investigated buildings: (left) plan view and (right) elevation view.

Three seismic sites in Italy were considered: Milan (MI), Naples (NA), and L'Aquila (AQ), associated with low, moderate, and high seismicity. For all sites, two soil conditions were implemented: type A and C, with an average velocity of the shear waves larger than 800 m/s and ranging in 180 – 360 m/s, respectively (Ministero delle Infrastrutture e dei Trasporti, 2018). Both damage limitation limit state (DLS) and life safety limit state (LSLS) were considered for designing the structural elements, where DLS and LSLS were associated with a return period (T_R) equal to 50 and 475 years, assuming a nominal life equal to 50 years and an II occupancy category (ordinary buildings) (Ministero delle Infrastrutture e dei Trasporti, 2018). The design was implemented by assuming a medium ductility class (CDB), considering Concrete C45/55 and steel B450C; the design process is described in detail in (Magliulo et al., 2023).

Capacity criteria and damage states

The investigated capacity criteria and damage states (DSs) are defined in Table 1, and the related capacity formulations are reported in Equations (1) to (8). In particular, EDP_{DS} defines the engineering demand parameter (EDP) associated with DS, and $EDP_{DS,c}$ is associated with the capacity EDP thresholds expressed for DS. Both EDP_{DS} and $EDP_{DS,c}$ were selected according to the latest literature studies in the field.

LS	DLS		LSLS					NCLS
DS	$DS_{IDR,NSD}$	$DS_{\theta y}$	$DS_{IDR,SD}$	$DS_{IDR,4\%}$	$DS_{\theta u}$	$DS_{Vbc,d}$	$DS_{Vbc,b}$	DS_{RDRu}
EDP_{DS}	IDR	θ	IDR	IDR	θ	Vbc	Vbc	RDR
$EDP_{DS,c}$	IDR_{NSD}	θ_y	IDR_{SD}	$IDR_{4\%}$	$\theta_{u,80\%}$	$V_{u,bc,d}$	$V_{u,bc,b}$	RDR_u
Eq.	(1)	(2)	(3)	(4)	(5)	(6)	(7)	(8)

Table 1. Investigated damage criteria and DSs associated with DLS, LSLS, and NCLS.

$DS_{IDR,NSD}$ defines the capacity associated with the failure of panel-to-structure cladding connection, referring the commonly used hammer-heat strap connection, according to (Zoubek

et al., 2016) and in compliance with (CEN, 2005); this damage criteria is associated with DLS, and it is implemented considering interstory drft ratio (IDR) as an EDP, according to Equation (1).

$$\mathrm{IDR_{NSD}} = 0.01 \tag{1}$$

$DS_{\theta y}$ is associated with the yielding chord rotation θ of the column, where this latter parameter is considered as an EDP. The formulation used for the identification of the capacity θ_y is defined in Equation (2), according to Fardis and Biskinis (Biskinis and Fardis, 2010; Fardis and Biskinis, 2003) and Fischinger et al. (Fischinger et al., 2008); the definition of the symbols can be found in the abovementioned studies.

$$\theta_y = \phi_y \cdot \frac{L_s}{3} + 0.00275 + a_{sl} \cdot \frac{\varepsilon_y}{d-d'} \frac{0.2 \cdot d_b \cdot f_y}{\sqrt{f_c}} \tag{2}$$

Both $DS_{IDR,NSD}$ and $DS_{\theta y}$ are correlated with DLS condition. IDR_{SD} is associated with severe structural damage ($DS_{IDR,SD}$) according to the criteria defined in the draft of the new Eurocode (CEN, 2020a, 2020b), where IDR is considered as an EDP. Equation (3) reports the related capacity criterion.

$$\mathrm{IDR_{SD}} = 0.02 \tag{3}$$

An higher capacity IDR threshold was also considered to assess (more) severe structural damage ($DS_{IDR,4\%}$), as it is reported in Equation (4).

$$\mathrm{IDR_{4\%}} = 0.04 \tag{4}$$

The ultimate chord rotation condition ($DS_{\theta u}$) was assessed considering the column chord rotation θ as an EDP, referring to the formulation developed by Haselton and Deierlein (Haselton and Deierlein, 2007) and Haselton et al. (Haselton et al., 2008), associated with a strength drop of 20% from the capping condition, as it is defined in Equation (5); the formulation of θ_c (capping rotation) and θ_{pc} (post-capping rotation) can be found in the abovementioned studies.

$$\theta_{u,80\%} = \theta_c + 0.2 \cdot \theta_{pc} \tag{5}$$

$DS_{Vbc,d}$ and $DS_{Vbc,b}$ are associated with ductile and brittle failure of the column-to-beam dowel connection, as it was defined by (Cimmino et al., 2020), and the related capacities, reported in Equations (6) and (7), respectively, are based on the assessment of the ultimate beam-column shear force $V_{u,bc}$. The capacity criteria were defined considering the minimum shear force over multiple damage criteria, as it is formulated in the abovementioned studies; the related correlations are not reported in this paper for the sake of brevity.

$$V_{u,bc,d} = \min\{V_{R,d,CNR}, V_{R,d,SC}, V_{R,d,EOTA,m}, V_{R,d,EOTA,c}, V_{R,d,VT,m}\} \tag{6}$$

$$V_{u,bc,b} = \min\{V_{R,b,SC}, V_{R,b,EOTA,m}, V_{R,b,EOTA,c}, V_{R,b,VT}, V_{R,b,ZFI}\} \tag{7}$$

IDR_{SD}, $DS_{IDR,4\%}$, $DS_{\theta u}$, $DS_{Vbc,d}$, and $DS_{Vbc,b}$ are compatible with LSLS. Finally, NCLS condition was assessed considering a significant inelastic deformation of the structure, close to a sidesway collapse condition, as it was discussed in (Camata et al., 2017; Magliulo et al., 2018; Ricci et al., 2018). Roof drift ration (RDR) was considered as an EDP, and the capacity criterion is reported in Equation (8), where RDR_c and V_h are the pushover capping RDR and shear force, respectively.

$$\mathrm{RDR_u} = \mathrm{RDR} > \mathrm{RDR_c}: V_h(\mathrm{RDR}) = 0.5 \max(V_h) \tag{8}$$

The seismic demands associated with the investigated LSs was derived from NTC 2018 (Ministero delle Infrastrutture e dei Trasporti, 2018) for DLS, LSLS, and NCLS, and two alternative NCLS demand threshold were derived from (CEN, 2005) and US codes (American Society of Civil Engineers, 2017; Luco et al., 2007). In particular, DLS (LSLS) spectral accelerations associated with the building period ($Sa(T_1)$) were equal to 0.034 and 0.082 g (0.107 and 0.212 g) for soil type A and C, respectively. The three alternative seismic demands associated with NCLS resulted in ($NCLS_1$) 0.146 and 0.261 g, ($NCLS_2$) 0.213 and 0.317 g, and ($NCLS_3$) 0.161 and 0.318 g for soil type A and C, respectively. Further details regarding the computation of the seismic demands can be found in (Magliulo et al., 2023). It should be noted that the building period T_1 was assumed to be equal to 2 s for all buildings, as this value was compatible with all case studies and was used to select the analysis loading histories, as it is discussed in the following section.

Numerical modelling and multiple stripe analysis

Three-dimensional models were implemented in OpenSees (McKenna et al., 2000), including columns and beams. The columns were fixed at their ends (socket foundation), and the beam to

column connections were modelled as hinges. A rigid diaphragm was assigned to the top horizontal elements, simulating the concrete slab. The beams were modelled as linear elastic, whereas the inelastic response was assigned to the columns through the lumped plasticity approach (Ricci et al., 2018). In particular, a series model was implemented for each column (Magliulo et al., 2023): (a) the Ibarra-Medina-Krawinkler (IMK) model (Ibarra et al., 2005; Ibarra and Krawinkler, 2005) was assigned to a zerolength rotational spring, connecting the fixed column end to a the internal column node, and (b) a linear elastic flexural response was assigned to a monodimensional element, connecting the abovementioned internal column node to the top column node. The backbone moment-rotation response associated with IMK model includes (a) a linear branch (up to yielding moment/rotation, (b) an hardening branch (up to capping moment), (c) a softening branch (up to residual moment), and (d) an indefinite perfectly plastic response (residual moment). The modelling parameters were derived from literature studies (Biskinis and Fardis, 2010; Fischinger et al., 2008; Haselton et al., 2008; Mander et al., 1988; Ricci et al., 2018). The formulation of IMK model and detailed modelling of the column are omitted for the sake of brevity, and the reader is referred to the cited studies.

Nonlinear static and response history analyses were carried out considering the geometric nonlinearities (P-Δ effects (Ercolino et al., 2018)). The former analysis was aimed at estimating the building capacities defined in Equation (8) (Ricci et al., 2018). The response history analyses were performed via a multiple stripe analysis (MSA) procedure (Jalayer, 2003; Scozzese et al., 2020), and the analysis loading histories were derived according to the conditional spectrum (CS) approach by Iervolino et al. (Iervolino et al., 2018, 2017); in particular, $Sa(T_1)$ was used as an IM, setting T_1 equal to 2 s, according to the modal analysis results (Magliulo et al., 2023). Ten IM levels (or stripes) were implemented, from 10 to 100.000 years, and a number of 20 record pairs was considered for each IM level. Figure 2 shows IM levels expressed in terms of $Sa(T_1)$ for the investigated case studies.

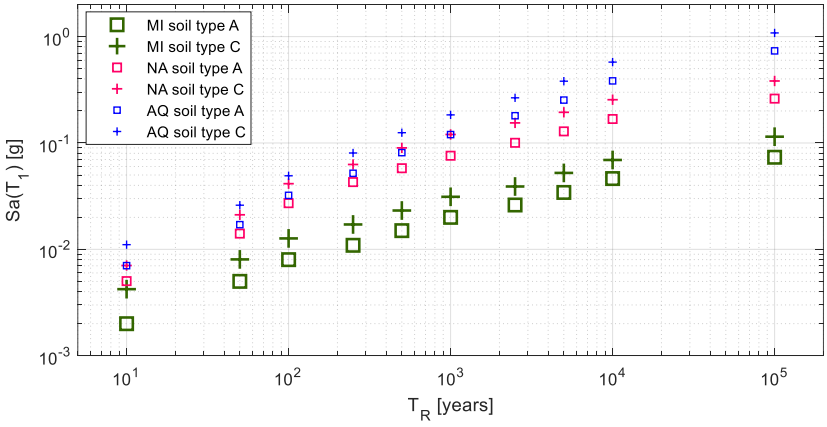

Figure 2. Spectral acceleration associated with building period ($Sa(T_1)$) for the investigated MSA IM levels.

Fragility assessment

The fragility of the investigated buildings was assessed considering multiple data analysis techniques, derived from well-established literature studies, i.e., Shome and Cornell (Shome and Cornell, 2000), maximum likelihood fit (Baker, 2015), normal probability paper fit (Cornell and Benjamin, 1970), and least squares fitting (Draper and Smith, 1998), discussed and used in several studies (Baraschino et al., 2020; Iervolino et al., 2023). Equation (9) reports the formulation related to the method developed by Shome and Cornell (Shome and Cornell, 2000), often referred to as three-parameter method, where j is the relevant IM level, P_C and P_{NC} define the probability of collapse and non-collapse, respectively, $\mu_{EDP_{DS,j}}$ and $\sigma_{EDP_{DS,j}}$ stand for mean and standard deviation of the distribution of $\ln(EDP_{DS,c})$. Shome and Cornell method provides discrete fragility measures.

$$\mathrm{F_{DS,j}} = P\left[EDP_{DS} \geq EDP_{DS,c} \mid \mathrm{Sa}(T_1) = |\mathrm{Sa}(T_1)|_j\right] = P_C + P_{NC}\left\{1 - \Phi\left[\frac{ln(EDP_{DS,c}) - \mu_{EDP_{DS,j}}}{\sigma_{EDP_{DS,j}}}\right]\right\} \quad (9)$$

The formulation associated with the maximum likelihood fit (MXL) method (Baker, 2015) is reported in Equation (10), where u is the number of analysis stripes, n is the number of analysis records, q_j is the number of failures associated with the j[th] stripe.

$$\{\mu_{DS}, \sigma_{DS}\} = \underset{\mu'_{DS}, \sigma'_{DS}}{argmax}\left[\sum_{j=1}^{u}\left\{ln\binom{n}{q_j} + q_j\, ln\left\{\Phi\left[\frac{\ln(|\mathrm{Sa}(T_1)|_j) - \mu'_{DS}}{\sigma'_{DS}}\right]\right\} + (n - q_j)\, ln\left\{1 - \Phi\left[\frac{\ln(|\mathrm{Sa}(T_1)|_j) - \mu'_{DS}}{\sigma'_{DS}}\right]\right\}\right\}\right] \quad (10)$$

The normal probability paper (NPP) fit method (Cornell and Benjamin, 1970) was implemented by fitting the Shome and Cornell fragility through a linear model. In particular, the fitting model is reported in Equation (11).

$$Z = -\frac{\mu_{DS}}{\sigma_{DS}} + {\sigma_{DS}}^{-1} \ln(\mathrm{Sa}(T_1)) \quad (11)$$

μ_{DS} and σ_{DS} can be assessed using Equations (12) and (13), respectively.

$$\sigma_{DS} = \frac{\sum_{j=1}^{u}(z_j - \bar{z})^2}{\sum_{j=1}^{p}(z_j - \bar{z})\left[\ln(|\mathrm{Sa}(T_1)|_j) - \overline{\ln(\mathrm{Sa}(T_1))}\right]} \quad (12)$$

$$\mu_{DS} = \overline{\ln(\mathrm{Sa}(T_1))} - \frac{\bar{z}}{\sigma_{DS}} \quad (13)$$

$\bar{z}$ and $\overline{\ln(\mathrm{Sa}(T_1))}$ can be computed using Equations (14) and (15), respectively; z_j defines failure probability associated with the j[th] stripe.

$$\bar{z} = u^{-1}\sum_{j=1}^{u} z_j \quad (14)$$

$$\overline{\ln(\mathrm{Sa}(T_1))} = u^{-1}\sum_{j=1}^{u} \ln\left(|\mathrm{Sa}(T_1)|_j\right) \quad (15)$$

The least squares fitting (LSF) method (Draper and Smith, 1998) is implemented by fitting Shome and Cornell fragilities, minimizing the squared error sum, according to Equation (16); in particular, P_{NC}, P_C, $\mu_{EDP_{DS,j}}$, and $\sigma_{EDP_{DS,j}}$ are estimated according to the Shome and Cornell method.

$$\{\mu_{DS}, \sigma_{DS}\} = \underset{\mu', \sigma'}{argmin}\left[\sum_{j=1}^{u}\left\{P_{NC}\left\{1 - \Phi\left[\frac{ln(EDP_{DS,c}) - \mu_{EDP_{DS,j}}}{\sigma_{EDP_{DS,j}}}\right]\right\} + P_C - \Phi\left[\frac{\ln(|\mathrm{Sa}(T_1)|_j) - \mu'_{DS}}{\sigma'_{DS}}\right]\right\}^2\right] \quad (16)$$

Results and concluding remarks

Figure 3 shows the fragility curves associated with the fitted fragility curves, considering the assessment techniques defined in the previous section. The curves are depicted for all AQ buildings scenarios and considering all DSs. MLF method overall provides the highest fragility and the lowest fitted uncertainty, especially for LSLS and NCLS. The sequence of DS curves associated with MXL is the same over the difference case studies (soil type and building geometry layout). The brittle failure of the dowel connection just precedes the nonstructural element damage, and this stresses the criticality of this failure mode, which should be absolutely avoided by providing adequate structural detailing (e.g., see (Cimmino et al., 2020)). The following achieved DSs, increasing the IM level, are conventional IDR-based structural damage (2% IDR), more severe IDR-based structural damage (4% IDR), and coinciding ductile failure of dowel connection, ultimate column chord rotation, and RDR-based sidesway collapse.

The fragility curves related to DLS DSs and IDR-based LSLS DSs estimated according to NPP and LSF are quite similar to the ones associated with MXL, even though some differences can be identified. For example, nonstructural damage fragility associated with NPP is slightly higher (lower) than the one related to MXL and NPP for soil C (A) conditions, and similar results are found regarding IDR-based structural damage DSs. For DSs associated with a relatively reduced number of collapses over only a stripe, i.e., for $DS_{\theta u}$, $DS_{Vbc,d}$, and DS_{RDRu}, a major discrepancy is found over the different methods, in terms of both median values and fitted uncertainty, and MXL tends to provide the most conservative fragilities, as it might have been expected.

It is interesting to notice that IDR-based significant damage defined in the draft of the new Eurocode (CEN, 2020a, 2020b), i.e., associated with 2% IDR, represents more an upper bound

condition with respect to DSL rather than being compatible with LSLS curves. This was expected since IDR equal to 2% is more comparable with yielding conditions of a (code-conforming) RC columns than with more severe damage conditions, as it can be found in the literature (Deyanova et al., 2014; Ercolino et al., 2016). Accordingly, verifying $DS_{IDR,SD}$ as a LSLS condition would result in an extremely severe and conservative requirement, not allowing the structure to take advantage of the inelastic capacities. Conversely, assuming IDR equal to 4% would result in a condition that is sufficiently more severe than DLS but, at the same time, conservatively ahead of heavily plastic conditions, e.g., ultimate chord rotation, or (ductile) failure of the dowel connection.

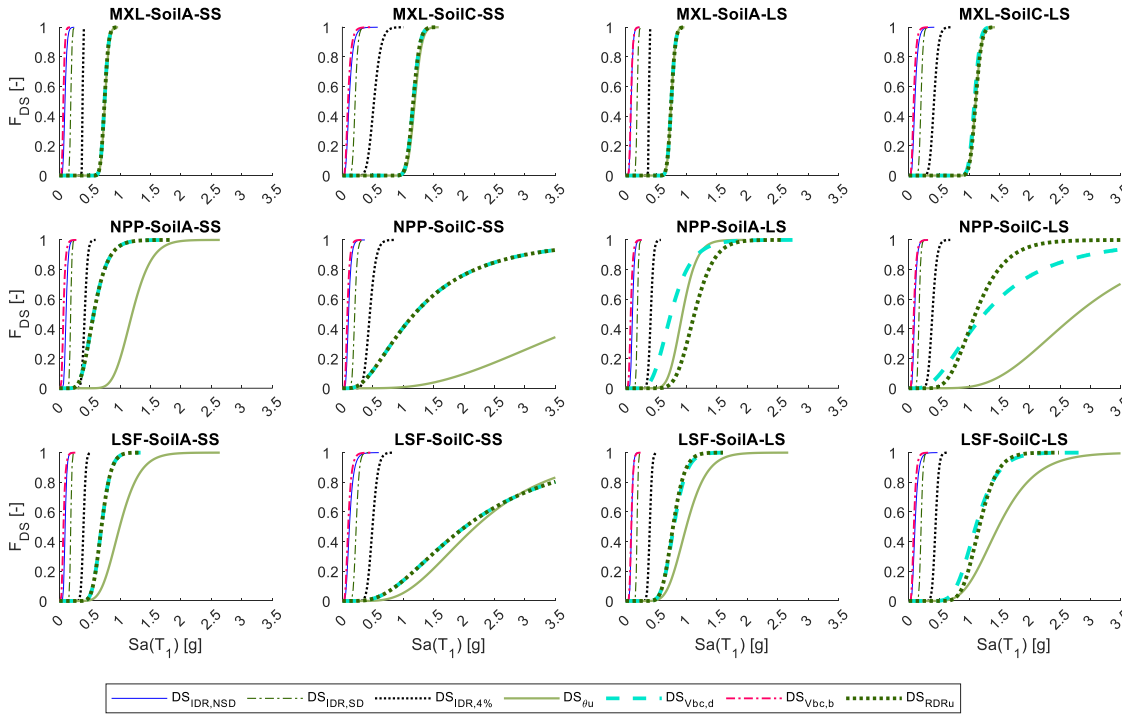

Figure 3. Fragility curves assessed considering three fitted methods for all DSs and AQ building scenarios (soil types A and B and building geometric layouts SS and LS).

The study provided a comprehensive assessment of the seismic fragilities of code-conforming single-story RC precast buildings. Several damage criteria were taken into account, as well as DLS, LSLS, and NCLS were considered. The investigated building scenarios are representative of common industrial buildings in Italy and Europe, and the findings of the study might be implemented or extended by researchers and practitioners for improving seismic design and assessment of one-story precast buildings. In particular, the influence of the seismic design provisions on the seismic capacity associated with multiple damage states was assessed, and the provided fragility curves, compared to seismic demand measures, potentially provides technical insights onto the efficiency of the abovementioned design process. However, the results of this study cannot be considered to be fully exhaustive, and further investigations should be carried out.

Acknowledgement

The project was funded by the Department of Civil Protection in the framework of the Re.LUIS 2022-2024 WP3 project. Authors thank Andrea Belleri, Davide Bellotti, Fabio Biondini, Bruno Dal Lago, Roberto Nascimbene, and Paolo Riva for the interesting discussions on the article topic.

References

American Society of Civil Engineers, 2017. Minimum Design Loads and Associated Criteria for Buildings and Other Structures, 7th ed. American Society of Civil Engineers, Reston, VA. https://doi.org/10.1061/9780784414248

Baker, J.W., 2015. Efficient Analytical Fragility Function Fitting Using Dynamic Structural Analysis. Earthquake Spectra 31, 579–599. https://doi.org/10.1193/021113EQS025M

Baraschino, R., Baltzopoulos, G., Iervolino, I., 2020. R2R-EU: Software for fragility fitting and evaluation of estimation uncertainty in seismic risk analysis. Soil Dynamics and Earthquake Engineering 132, 106093. https://doi.org/10.1016/j.soildyn.2020.106093

Biskinis, D., Fardis, M.N., 2010. Flexure-controlled ultimate deformations of members with continuous or lap-spliced bars. Structural Concrete 11, 93–108. https://doi.org/10.1680/stco.2010.11.2.93

British Standards Institution, European Committee for Standardization, 2005. Eurocode 8, design of structures for earthquake resistance. British Standards Institution, London.

Camata, G., Celano, F., De Risi, M.T., Franchin, P., Magliulo, G., Manfredi, V., Masi, A., Mollaioli, F., Noto, F., Ricci, P., Spacone, E., Terrenzi, M., Verderame, G., 2017. Rintc Project: Nonlinear Dynamic Analyses Of Italian Code-Conforming Reinforced Concrete Buildings For Risk Of Collapse Assessment, in: Proceedings of the 6th International Conference on Computational Methods in Structural Dynamics and Earthquake Engineering (COMPDYN 2015). Presented at the 6th International Conference on Computational Methods in Structural Dynamics and Earthquake Engineering Methods in Structural Dynamics and Earthquake Engineering, Institute of Structural Analysis and Antiseismic Research School of Civil Engineering National Technical University of Athens (NTUA) Greece, Rhodes Island, Greece, pp. 1474–1485. https://doi.org/10.7712/120117.5507.17050

CEN, 2020a. draft of new EN 1998–3. Eurocode 8: Design of structures for earthquake resistance - Part 3: Assessment and retrofitting of buildings.

CEN, 2020b. draft of new EN 1998–1-2. Eurocode 8: Design of structures for earthquake resistance - Part 1-2: Rules for new buildings.

CEN, 2005. EN 1998–3. Eurocode 8: Design of structures for earthquake resistance - Part 3: Assessment and retrofitting of buildings.

Cimmino, M., Magliulo, G., Manfredi, G., 2020. Seismic collapse assessment of new European single-story RC precast buildings with weak connections. Bull Earthquake Eng. https://doi.org/10.1007/s10518-020-00952-7

Clementi, F., Scalbi, A., Lenci, S., 2016. Seismic performance of precast reinforced concrete buildings with dowel pin connections. Journal of Building Engineering 7, 224–238. https://doi.org/10.1016/j.jobe.2016.06.013

Consiglio Superiore dei Lavori Pubblici (CS.LL.PP.), 2008. D.M. del 14/01/2008 – “Norme tecniche per le Costruzioni 2008”. NTC 2008 (in Italian).

Cornell, C.A., Benjamin, J.R., 1970. Probability, Statistics and Decision for Civil Engineers. McGraw-Hill, New York, NY.

Deyanova, M., Pampanin, S., Nascimbene, R., 2014. Assessment of single-storey precast concrete industrial buildings with hinged beam-column connections with and without dowels, in: Proceedings of Second European Conference on Earthquake Engineering and Seismology. EAEE, Istanbul, pp. 1–14.

Draper, N.R., Smith, H., 1998. Applied Regression Analysis, Third edition. ed. John Wiley & Sons, New York, NY.

Ercolino, M., Magliulo, G., Manfredi, G., 2016. Failure of a precast RC building due to Emilia-Romagna earthquakes. Engineering Structures 118, 262–273. https://doi.org/10.1016/j.engstruct.2016.03.054

Ercolino, M., Petrone, C., Magliulo, G., Manfredi, G., 2018. Seismic Design of Single-Story Precast Structures for *P* -Δ Effects. ACI Structural Journal 115. https://doi.org/10.14359/51701915

Fardis, M.N., Biskinis, D., 2003. Deformation capacity of RC members, as controlled by flexure or shear, in: Otani Symposium. pp. 511–530.

Fischinger, M., Kramar, M., Isaković, T., 2008. Cyclic response of slender RC columns typical of precast industrial buildings. Bull Earthquake Eng 6, 519–534. https://doi.org/10.1007/s10518-008-9064-7

Haselton, C.B., Deierlein, G.G., 2007. Assessing Seismic Collapse Safety Of Modern Reinforced Concrete Moment Frame Buildings (No. 156). The John A. Blume Earthquake Engineering Center. Department of Civil and Environmental engineering. Stanford University, Stanford CA.

Haselton, C.B., Liel, A.B., Taylor-Lange, S., Deierlein, G.G., 2008. PEER Report No. 2007/03. Beam-column element model calibrated for predicting flexural response leading to global collapse of RC frame buildings (No. Report No. 2007/03). Pacific Earthquake Engineering Research Center, University of California, Berkeley, CA.

Ibarra, L.F., Krawinkler, H., 2005. Global collapse of frame structures under seismic excitations (No. 152). The John A. Blume Earthquake Engineering Center. Department of Civil and Environmental engineering. Stanford University, Stanford CA.

Ibarra, L.F., Medina, R.A., Krawinkler, H., 2005. Hysteretic models that incorporate strength and stiffness deterioration. Earthquake Engng Struct. Dyn. 34, 1489–1511. https://doi.org/10.1002/eqe.495

Iervolino, I., Baraschino, R., Belleri, A., Cardone, D., Della Corte, G., Franchin, P., Lagomarsino, S., Magliulo, G., Marchi, A., Penna, A., Viggiani, L.R.S., Zona, A., 2023. Seismic Fragility of Italian Code-Conforming Buildings by Multi-Stripe Dynamic Analysis of Three-Dimensional Structural Models. Journal of Earthquake Engineering 1–34. https://doi.org/10.1080/13632469.2023.2167889

Iervolino, I., Dolce, M., 2018. Foreword to the Special Issue for the RINTC (The Implicit Seismic Risk of Code-Conforming Structures) Project. Journal of Earthquake Engineering 22, 1–4. https://doi.org/10.1080/13632469.2018.1543697

Iervolino, I., Spillatura, A., Bazzurro, P., 2018. Seismic Reliability of Code-Conforming Italian Buildings. Journal of Earthquake Engineering 22, 5–27. https://doi.org/10.1080/13632469.2018.1540372

Iervolino, I., Spillatura, A., Bazzurro, P., 2017. Rintc Project - Assessing The (Implicit) Seismic Risk Of Code-Conforming Structures In Italy, in: Proceedings of the 6th International Conference on Computational Methods in Structural Dynamics and Earthquake Engineering (COMPDYN 2015). Presented at the 6th International Conference on Computational Methods in Structural Dynamics and Earthquake Engineering Methods in Structural Dynamics and Earthquake Engineering, Institute of Structural Analysis and Antiseismic Research School of Civil Engineering National Technical University of Athens (NTUA) Greece, Rhodes Island, Greece, pp. 1545–1557. https://doi.org/10.7712/120117.5512.17282

Jalayer, F., 2003. Direct Probabilistic seismic analysis: implementing nonlinear dynamic assessment (PhD thesis). Department of Civil and Environmental Engineering, Stanford University, Stanford CA.

Luco, N., Ellingwood, B.R., Hamburger, R.O., Hooper, J.D., Kimball, J.K., Kircher, C.A., 2007. Risk-targeted versus current seismic design maps for the conterminous United States, in: SEAOC 2007 CONVENTION PROCEEDINGS.

Magliulo, G., Bellotti, D., Cimmino, M., Nascimbene, R., 2018. Modeling and Seismic Response Analysis of RC Precast Italian Code-Conforming Buildings. Journal of Earthquake Engineering 22, 140–167. https://doi.org/10.1080/13632469.2018.1531093

Magliulo, G., D'Angela, D., Piccolo, V., Di Salvatore, C., Caterino, N., 2023. Seismic capacity and performance of code-conforming single-story RC precast buildings considering multiple limit states and damage criteria. Journal of Building Engineering 70, 106316. https://doi.org/10.1016/j.jobe.2023.106316

Mander, J.B., Priestley, M.J.N., Park, R., 1988. Theoretical Stress-Strain Model for Confined Concrete. J. Struct. Eng. 114, 1804–1826. https://doi.org/10.1061/(ASCE)0733-9445(1988)114:8(1804)

McKenna, F., Fenves, G.L., Scott, M.H., 2000. OpenSees: Open System for Earthquake Engineering Simulation. Pacific Earthquake Engineering Research Center. University of California,Berkeley, CA. Available at: http://opensees.berkeley.edu.

Ministero delle Infrastrutture e dei Trasporti, 2018. D.M. del 17/01/2018 – "Aggiornamento delle Norme tecniche per le Costruzioni 2018" NTC 2018 (in Italian).

Ozden, S., Akpinar, E., Erdogan, H., Atalay, H.M., 2014. Performance of precast concrete structures in October 2011 Van earthquake, Turkey. Magazine of Concrete Research 66, 543–552. https://doi.org/10.1680/macr.13.00097

Ricci, P., Manfredi, V., Noto, F., Terrenzi, M., Petrone, C., Celano, F., De Risi, M.T., Camata, G., Franchin, P., Magliulo, G., Masi, A., Mollaioli, F., Spacone, E., Verderame, G.M., 2018. Modeling and Seismic Response Analysis of Italian Code-Conforming Reinforced Concrete Buildings. Journal of Earthquake Engineering 22, 105–139. https://doi.org/10.1080/13632469.2018.1527733

RINTC Workgroup, 2018. Results of the 2015-2017 Implicit seismic risk of code-conforming structures in Italy (RINTC) project. (Technical Report and Deliverables). Rete dei Laboratori Universitari di Ingegneria Sismica (ReLUIS), Naples.

Scozzese, F., Tubaldi, E., Dall'Asta, A., 2020. Assessment of the effectiveness of Multiple-Stripe Analysis by using a stochastic earthquake input model. Bull Earthquake Eng 18, 3167–3203. https://doi.org/10.1007/s10518-020-00815-1

Shome, N., Cornell, C.A., 2000. Structural Seismic Demand Analysis: Consideration of "Collapse," in: Proceedings of 8th ACSE Specialty Conference on Probabilistic Mechanics and Structural Reliability. Presented at the 8th ACSE Specialty Conference on Probabilistic Mechanics and Structural Reliability, South Bend, Indiana.

Toniolo, G., Colombo, A., 2012. Precast concrete structures: the lessons learned from the L'Aquila earthquake. Structural Concrete 13, 73–83. https://doi.org/10.1002/suco.201100052

Zoubek, B., Fischinger, M., Isaković, T., 2016. Cyclic response of hammer-head strap cladding-to-structure connections used in RC precast building. Engineering Structures 119, 135–148. https://doi.org/10.1016/j.engstruct.2016.04.002